

# Improved understanding of combined sewer systems using the Illinois Conveyance Analysis Program (ICAP)

Nils Oberg<sup>1\*</sup>, Arthur R. Schmidt<sup>1</sup>, Blake J. Landry<sup>1</sup>, Arturo S. Leon<sup>1,2</sup>, Andrew R.  
Waratuke<sup>1</sup>, José M. Mier<sup>1</sup>, and and Marcelo H. García<sup>1</sup>

<sup>1</sup>University of Illinois, 205 N Mathews Ave, Urbana, IL 61801

<sup>2</sup>University of Houston, Civil and Environmental Engineering, Room N107, 4726  
Calhoun Road, Houston TX 77204

\*corresponding author; nils@obergs.net

‘The Version of Record of this manuscript has been published and is available in Journal of Applied Water Engineering and Research, Published online 16 Feb 2017. <http://www.tandfonline.com/doi/full/10.1080/23249676.2017.1287017>

## Abstract

Understanding the conveyance of sewer networks is vital, especially in cases of great variability in flow rates, such as in combined sanitary and storm sewer systems. Conventional conveyance studies in sewer systems often have extended computation times due to complexity of the solution, or alternatively make assumptions that ignore the water-surface profile within a pipe. In previous research, the hydraulic performance graph (HPG) was successfully used for open-channel capacity determination. The HPG summarizes the results of many backwater calculations for a reach so that these calculations do not need to be repeated. This article describes algorithms utilized by the Illinois Conveyance Analysis Program that uses the HPGs to describe the conveyance of a system, identify bottlenecks for varying conditions, conserve mass by tracking outflow and overflows under stepwise steady flow conditions. The software is freely available at <https://github.com/obergshavefun/icap/wiki>.

Keywords: CSO; Conveyance analysis; Combined sewer systems; Bottleneck analysis; Hydraulic performance graph; Open source

## Introduction

Sewer systems are ubiquitous in urban areas and are used to convey flow from a point source to a treatment destination. Combined sewer systems are networks in which both sanitary and storm flows are conveyed to the same destination (Tibbetts, 2005). Within the United States, there are 772 municipalities that have combined sewer systems (U.S. EPA, 2016) that have the potential to overflow and pollute waterways. When studying the conveyance capacity of these systems, analyses often divide the system into reaches delimited by manholes or junctions, effectively ignoring the water-surface profile within a pipe (Rossman, 2008). In large systems with long pipes, this assumption ignores backwater effects thus potentially introducing significant errors. In another approach, the conveyance capacity can be determined by performing calculations using the Saint-Venant equations for each conduit in the system for every flow condition (Franz and Melching, 1997; Wallingford Software, 2002; Danish Hydraulics Institute, 2009; Brunner, 2010). This is not unreasonable for problems in which a small number of flows are considered. In a large sewer system, a large range of flows and boundary conditions is possible due to spatial extent and system topology. In addition, developing operational rules or making operational decisions for sewer systems can require extensive simulation to account for varying storage conditions. This results in a large number of combinations of inflow and boundary conditions that need to be considered. In closed-conduits, both free-surface and pressurized flow conditions (i.e., mixed flow conditions) can exist within the system and even within the same pipe. This additional complexity reduces the number of combinations of inflows and boundary conditions that can be simulated in a given time frame.

In previous research, the hydraulic performance graph (HPG) was successfully used for open-channel conveyance capacity determination in both gradually varied and unsteady flow conditions (González-Castro and Yen, 2000b; Leon et al., 2013; Gibson et al., 2014; Leon et al., 2014). The HPG summarizes the results of backwater calculations for a reach so that these calculations do not need to be repeated. Further work on the HPG resulted in the incorporation of HPGs for closed conduits for both free surface flows (Hoy, 2005) and pressurized flows (Zimmer et al., 2013) in unsteady flow conditions. A proof-of-concept model was developed by Oberg et al. (2006) that uses the HPG to compute steady-state conditions in closed conduits, incorporating a transition from free-surface to pressurized flow conditions. This article expands on Oberg et al. (2006) by incorporation of mass-conservation, pumping outflows, dynamic junction-loss computations, and packaging of the algorithms into a standalone desktop graphical user interface-based software program called the Illinois Conveyance Analysis Program (ICAP). The ICAP model allows users to describe the conveyance of all components of a system, identify bottlenecks for different inflows and boundary conditions, conserve mass by tracking of overflows and outflows, all under stepwise steady flow conditions for rapid analysis. The ICAP model can provide information necessary to make operational decisions and identify system retrofits that will identify and

eliminate the most restrictive bottlenecks (Yen and Mays, 2001) and maximize the conveyance capacity of the system. In addition to the application to combined sewer systems, ICAP can also be used in any system for which HPGs are available. Using a HPG utility (Landry and Oberg, 2016) or algorithms presented by Schmidt (2002), HPGs can be created for non-prismatic open channels such as those found in natural rivers and canals. ICAP can be configured to use these HPGs, which are treated the same way as HPGs that are created for closed-conduit pipe networks.

## Background and Assumptions

The ICAP program described in this article provides a framework to analyze the conveyance and volumetric performance of a system. The conveyance capacity of a system is defined as the maximum discharge that it can convey for a given set of boundary conditions without overflow at any point in the system (Yen and Mays, 2001). To determine these parameters, ICAP utilizes a hydraulic performance graph (HPG) for the computations in each reach. For some conditions described later, a mass balance computation is applied instead of the HPG; the computation relies on the storage of reservoirs and reaches but does not account for storage in shafts or manholes. In addition, the downstream boundary can be a shaft, a reservoir, a free-overfall, or a constant stage boundary. Finally, the network of reaches must be dendritic, meaning that a unique path exists between any two points in the system. This latter is not a limitation of the HPG method as this method could be extended to looped networks (Leon et al., 2013).

### *Hydraulic Performance Graph*

The free-surface relationship between upstream stage, downstream stage, and discharge is non-linear and is described by the gradually varied flow equation:

$$\frac{\partial y}{\partial t} = \frac{S_o - S_f}{1 - Fr^2}, \quad (1)$$

where

$$Fr = \frac{Q}{A\sqrt{yD}}; \quad (2)$$

$$S_f = \left( \frac{Qn}{k_s R^{2/3} A} \right)^2, \quad (3)$$

where

$$k_s = \begin{cases} 1.486, & \text{U.S. Customary System of Units} \\ 1.00, & \text{International System of Units,} \end{cases}$$

and  $S_o$  is the bed slope,  $Q$  is the discharge,  $n$  is the Manning’s “ $n$ ” roughness coefficient,  $R$  is the hydraulic radius,  $A$  is the area, and  $D$  is the hydraulic depth. The derivation of the gradually-varied flow equation originates in the momentum equation included in the Saint Venant equations. From the gradually-varied flow equation it can be shown that, for steady subcritical flow, there is a unique discharge for any given combination of downstream and upstream depths. Henderson (1966) and Xia and Yen (1992) discussed the magnitude of the various terms in the momentum equation and indicated that the two terms related to unsteady (i.e., dynamic flows) are of the same order as each other, are opposite in sign to each other, and usually will be much smaller than the other terms. Hence, other than for highly-variable conditions such as hydraulic transients or dam-break flows, neglecting the terms related to unsteady flows is reasonable and results in errors smaller than the uncertainty that arises from treating the flow as one-dimensional. Starting with these equations, the foundation for the HPG was laid in the development of delivery curves for mild-slope open channels (Bahkmeteff, 1932).

Chow (1959) extended the applicability of delivery curves to steep-slope open channels. Later the concept was extended to open channels with steep, horizontal, and adverse slopes, and expanded to develop the hydraulic performance graph (Yen and González-Castro, 1994; Yen and Mays, 2001). In addition, methods were developed for applying the HPG to unsteady-flow routing in open channels (González-Castro and Yen, 2000a) as well as to unsteady free-surface flow (Hoy, 2005; Leon et al., 2013; Gibson et al., 2014; Leon et al., 2014) and pressurized flows (Zimmer et al., 2013) in circular closed conduits.

There are three characteristic curves in an HPG for a prismatic section: Z-line, N-line, and C-curve. The Z-line represents horizontal water surface along the channel reach, the N-line denotes reachwise normal flow, and the C-curve indicates flow with critical depth at the exit (channels with mild slope) or at the entrance (channels with steep slope) of the reach. In addition, multiple hydraulic performance curves (HPC) are included in the HPG. Each HPC represents the downstream-upstream stage relationship for a given flow. The format of the graph allows for rapid inspection of the corresponding upstream stage for a given flow and downstream stage; Figure 1 illustrates a complete HPG. The HPG can be treated as a “black box”, functionally allowing the upstream depth to be interpolated from the downstream depth  $y_{\text{down}}$  and flow  $Q$  using the relationship given in Equation 4.

$$y_{\text{up}} = \text{HPG}(Q, y_{\text{down}}) \quad (4)$$

The interpolation procedure will be described in detail in the *Steady-State Routing* section (refer to page 7).

[Figure 1 about here.]

### ***Construction***

The organization of the curves comprising the HPG facilitates interpolation, resulting in increased computational efficiency. The procedure for the construction of HPGs in subcritical flow conditions for different types of slope channels has been documented in detail by Schmidt (2002). In essence, this procedure involves computing backwater profiles in the subcritical gradually-varied flow regime using a given downstream condition and flow rate. In addition to providing upstream values for the HPG, the backwater profiles allow determination of volume within a given reach for a particular profile. The volumetric performance graph (VPG) is computed during the HPG computation process and is a series of curves of constant discharge, each corresponding to the discharge for each HPC in the HPG. Each of these volumetric performance curves (VPC) in the VPG provide a downstream stage to reach volume relationship for a given flow. The VPG is essential in determining the volume for a given water surface profile during a simulation.

In closed conduits construction of each HPC and VPC has two separate components: free-surface and pressurized components. Downstream stages in the free-surface component are varied between critical depth and a certain downstream stage,  $y_{d_{\text{Max}}}$ , that causes the upstream end of the backwater profile computation to exceed a certain fraction  $f_f$  of full depth. In circular conduits with unit depths  $y/D$  greater than 0.8 the water surface is very unstable (Hamam and McCorquodale, 1982); thus for the purposes of this paper  $f_f = 0.8$ . For steep conduits, critical depth serves as the upstream boundary condition; the upstream boundary condition is varied and ends when the downstream depth is greater than  $f_f$  of full depth. For all conduits a pressurized counterpart,  $f'_f$ , is defined as a value greater than a fraction full of 1.0 and is applied to smooth instabilities during the transition from free-surface to pressurized conditions. For this paper,  $f'_f = 1.2$ .

### ***Pressurized Extension***

The second component in construction of a HPC for a closed conduit is the pressurized extension which facilitates lookup of both of free-surface and pressurized conditions within the same HPG. The HPC is extended by adding a line starting at  $f'_f$  times the diameter and extending to 100 times the diameter. The line represents

the downstream water surface elevation plus the head loss in a pressurized conduit which is computed by rearranging Manning’s formula in terms of  $h_f$ :

$$h_f = \frac{n^2 Q^2 L P^{4/3}}{k_s^2 A^{10/3}}. \quad (5)$$

where  $L$  is the length of the reach,  $P$  is the wetted perimeter, and the remainder of the variables are defined as in Equation 3. Since  $A$  and  $P$ , are constant,  $S_f$  is also constant. Therefore,  $h_f$  is constant for any  $Q$  regardless of the downstream stage. Since  $y_{\text{up}} = y_{\text{down}} + h_f$  the HPC line for pressurized flow is a 45° line.

Upstream flow depths that are in the transitional region  $f_f \leq y/D \leq f'_f$  are linearly interpolated since conditions with the conduit are highly variable. Interpolation relaxes the problem by not requiring the program to directly compute the local, transient effects of transitioning between regimes. The effect of ignoring these instabilities are assumed to be negligible since for conveyance analyses the time steps of the model are orders of magnitude greater than the time scale of transient effects.

### ***Temporal Assumption***

Under steady-state conditions, there is no volume change in time for a given reach, which can be mathematically represented as the following:

$$\frac{\partial Q}{\partial x} + \frac{\partial A}{\partial t} = q, \quad (6)$$

where  $q$  is lateral inflow (Chow et al., 1988). While a steady-state analysis has some value (e.g., design), many systems, such as combined sewer systems, are subject to varying inflow conditions. In ICAP, a stepwise steady approach is used which implies that at any time step, longitudinal change in flow is equal to any inflows in the reach. This approach is not as accurate as dynamic wave approximation unsteady flow routing; however, it is more accurate than routing using a kinematic wave approach since downstream boundary conditions are accounted for. The stepwise steady approach facilitates the analysis of system conveyance with time-varying input hydrographs such as those occurring during storm events, while reducing computational complexity by using the HPG lookup tables rather than calculating the momentum equation for each spatial- and time-step. Time-varying inflow hydrographs are approximated as a series of discrete steady flow profiles, with each profile corresponding to a specific time and having a constant flow for that time window.

## **Methodology**

The HPG by itself provides a tool for analyzing the conveyance and hydraulic behavior for a given reach. The steps for conveyance analysis for a pipe network are presented below (see also Figure 1 in the supplementary material).

- (1) Initialize simulation parameters.
- (2) For each time step, establish the flow in each pipe which is the sum of all upstream inputs.
- (3) Starting at downstream boundaries, calculate the water depths upstream using HPGs or volume balance computations depending on conditions.
- (4) Update the water depth at the downstream boundary condition based on how much water has entered or exited the system over the time step.
- (5) Repeat steps 2 to 4 until the simulation is completed.

Required inputs to the methodology include:

- Dendritic pipe network geometry, node parameters (such as overflow elevation), and junction-node connectivity.

- Inflow hydrographs representing surface runoff and sewer loads at specific locations in the pipe network; these are computed by an external hydrologic model and are linked to the simulation through the user interface.
- Initial condition of the simulation, possibly representing a partially-filled reservoir as a downstream boundary.
- Pumping parameters for long-term simulations.

### ***Step 1: Initialize Simulation***

In ICAP, HPGs are created one time for a given geometry configuration and are saved using both natural flow (e.g., upstream to downstream) and reverse flow (e.g., downstream to upstream) directions. When a simulation is started, these HPGs are loaded into computer memory. Piecewise cubic splines are created for interpolating between points on a curve. These splines represent a curve with a collection of third-order polynomials corresponding to intervals of the curve and have the property that the first derivative is continuous between intervals. Also during initialization, the total system volume curve  $F_{VT}$  is computed and loaded into memory. This curve denotes the system stage-storage relationship between the minimum and maximum possible elevations, assuming a horizontal water surface. This is useful in the special case that the downstream boundary invert is not the lowest point in the system (as is the case in the application below). In addition, ICAP utilizes the curve to simulate the effect of pumping by removing water from the system when inflows are not present.

### ***Step 2: Propagate Flows***

Under the stepwise steady assumption, flows for a given timestep are propagated to the downstream boundary. Flows in the pipe are initialized to zero and then starting at every inflow point, a traversal is made to the downstream boundary, adding the flow from the inflow point to the current flow in each pipe (see also Figure 1 in the supplementary material).

### ***Steps 3 and 4: Routing***

There are two primary modes of operation in ICAP modeling of systems. The first condition is referred to as static routing, and refers to conditions when there is no flow in the system and the hydraulic grade line is horizontal throughout the system. The second is referred to as steady-state routing and refers to conditions when flow is entering the system and HPGs are used to determine the hydraulic grade line throughout the conduits. In either condition, ICAP conserves volume by keeping count of the various volumetric components in the following variables:

- $V_I$ : total volume that has entered the system over the previous time-steps
- $v_i$ : the volume entered the system at the current time-step
- $V_P$ : the total volume that has left the system from pumping over previous time-steps
- $v_p$ : the volume that has left the system from pumping at the current time-step
- $V_O$ : the total volume that has overflowed the system over previous time-steps
- $v_o$ : the volume that has overflowed the system at the current time-step
- $v_t$ : the volume stored in the conduits at the current time-step
- $V_{\max}$ : the total volume that the system can hold

The mass balance procedure also accounts for overflows, which can be created by large rainfall events in combined sewer systems. At any given time, the overflow volume  $v_o = (V_I + v_i) - (V_P + v_p) - V_{\max}$ . If  $v_o$  is positive then an overflow has occurred and  $v_o$  is subtracted from  $v_i$  and added to  $V_O$ .

### Static Routing

When there are negligible inflows to the system, the hydraulic grade line is assumed to be horizontal. During these periods, ICAP can be configured to simulate pumping via a constant outflow rate or a variable time series outflow hydrograph. This pseudo-pumping routine removes water from the system by adding the pumped volume  $v_p$  at the current time-step to the total pumped  $V_P$ . Since the volume in the system at the current time step is known by  $(V_I + v_i - v_o) - (V_P + v_p)$ , the horizontal hydraulic grade line can be determined from the total system volume curve  $F_{VT}$ . This hydraulic grade line is used to update the downstream boundary water depth for the next time-step. Using the  $F_{VT}$  curve facilitates modeling of the special case where the downstream boundary is higher than the lowest point in the system, and the downstream boundary is dry but volume is present in lowest points, such as occurs in the case study. Pseudo-pumping is not applicable with the free-overfall and fixed-stage downstream boundary condition.

### Steady-State Routing

After flows are established, depths are propagated upstream starting at the downstream boundary. Since the HPG encapsulates both free and pressurized conditions, the upstream depth is interpolated from the HPG by using the flow in the current pipe and the downstream depth of the pipe. The downstream depth is either obtained from the upstream depth in the conduit immediately downstream, or from the boundary conditions if there are no downstream pipes. In a HPG, curves can be subcritical (mild, adverse, and horizontal slope), pressurized, and supercritical. Since the flow conditions can vary, the upstream depth computation also varies depending on the flow condition, as shown in Table 1. When applying the methodology to open-channel conduits such as rivers, the pressurized elements in the computation are neglected.

[Table 1 about here.]

Once water depth is determined in every conduit, the volume in the conduits is computed based on the VPG curves. If the downstream boundary is a storage reservoir, the volume stored in the reservoir at the current time is computed as  $v_r = (V_I + v_i) - (V_P + v_p) - v_t$ , where  $v_t$  is the volume stored in the conduits at the current time, and  $v_r$  is the volume in the downstream boundary.  $v_r$  is used in combination with a stage-storage curve to obtain a starting water depth for the next time-step. If the downstream boundary is a fixed-stage or free-overfall type, the volume computation is not applicable and the given boundary condition is applied (for example, critical depth or fixed stage).

### HPG Interpolation

Interpolation is used to obtain upstream depths when the downstream flow and depth do not exactly coincide on a HPC. The upstream depth is linearly interpolated as

$$y_{up} = u_l + \frac{Q - Q_l}{Q_u - Q_l} |u_l - u_u|,$$

where  $u_l$  and  $u_u$  are the upstream depths on the lower and upper bracketing curves, respectively.  $Q_l$  and  $Q_u$  are the flow rates corresponding to the lower and upper bracketing curves, and  $Q$  is the input downstream flow.

### Junction Loss Computation

When a junction between conduits occurs, there is an associated loss due to merging flows or expansion or contraction of the conduit. This energy loss is accounted for within the ICAP program by the energy equation (Equation (7)) for each upstream branch in a junction,

$$\frac{p_i}{\gamma} + z_i + \frac{V_i^2}{2g} = \frac{p_o}{\gamma} + z_o + \frac{V_o^2}{2g} + K \frac{|V_o| V_o}{2g}, \quad (7)$$

where  $p$  is the pressure head,  $z$  is the pipe invert,  $V$  is the velocity,  $g$  is the gravitational constant, and  $\gamma$  is the specific weight.  $K$  is computed individually for the main upstream segment ( $K_M$ ) and lateral upstream segment ( $K_L$ ) using Equations 16.11 and 16.12, respectively, from Hager (1999):

$$K_M = (\mu^{-1} - 1)^2 - 1 + 3q - 2q^2; \quad (8)$$

$$K_L = (\mu^{-1} - 1)^2 + q - 2q^2, \quad (9)$$

where  $q$  is the ratio of the flow in the upstream main segment to the flow in the downstream segment, and  $\mu$  is defined using Equation 16.6 from Hager (1999),

$$\mu^{-1} = \left( 1 + \left[ (1-q)(2-q) \left( 1 - \frac{2}{3} \cos \alpha - \frac{1}{3} \cos^2 \alpha \right) + \frac{1}{9} \cos^2 \alpha \right]^{1/2} \right) \left( 1 + \frac{1}{3} \cos \alpha \right)^{-1}, \quad (10)$$

where  $\alpha$  is the angle of location (e.g., the angle between the lateral and main branches). Equations (9) and (8) are iteratively computed for each junction in the system during the course of steady-state routing. (See Figure 2 in the supplemental material for an example junction configuration.)

### *Software*

To facilitate ease-of-use, a Microsoft Windows based user interface was developed for ICAP as shown in Figure 2. The GUI is based on the EPA SWMM 5 user interface (Rossman, 2008) with significant modifications. The tool enables a user to draw the conduit network including junctions, conduits, and storage units as well as to provide simulation and geometric parameters. Results can be visualized in tabular, graphical, and statistical format including profile plots of paths within a conduit network. The software has been made available both in binary executable (i.e. ready-to-run) and source code form at <https://github.com/obergshavefun/icap/wiki>. Also included on the website is an example dataset and tutorial guide that users can use to get started. Version 1.6 of the program and associated tutorial and example data are permanently located at <http://hdl.handle.net/2142/89288>.

[Figure 2 about here.]

## **Application**

A large dendritic pipe system and reservoir, depicted in Figure 3 (a), is designed to capture and store combined sewer overflows (CSO) during large storm events as part of a CSO remediation project. Pipes range in diameter from 8 feet [2.4 m] to 33 feet [10.1 m] and are up to 300 feet [91.4 m] below the ground surface. The storage capacity of the 38 miles [61.2 km] of pipe system is 0.5 billion gallons [1,900,000 m<sup>3</sup>], while the reservoir has a storage capacity of 7 billion gallons [26,000,000 m<sup>3</sup>]. Each inflow location is a dropshaft at which flow-rate into the system can be throttled. In this application, two aspects of system performance are analyzed. The first aspect concerns conveyance capacity during events on the order of days; an analysis of this kind can yield an understanding of the behavior of the system and facilitate alternative operations. The second aspect concerns the storage performance of the system, and the duration of the analysis is on the order of months.

### *Conveyance Analysis*

In the system illustrated in Figure 3 (a), during certain events conveyance capacity is reduced due to a combination of adverse slope tunnels, and head losses at junctions due to large merging inflows. The system includes a large reservoir (C) at elevation -297.5 ft [-90.7 m], a central junction (J) at elevation -320 ft [-97.5 m] and additional locations at elevation -224 ft [-68.3 m] (B) and -154 ft [-46.9 m] (A); B represents a location where



the diameter changes and A represents the upstream-most location. Initial conditions for the system are dry conditions with the reservoir empty. A profile plot of tunnels ABJC at 20 hours into the simulation, as shown in Figure 3 (b), shows that conveyance is greatly reduced around junction J and through JC. The profile plot graphs the geometric properties of the conduits (e.g., pipe invert and crown elevations), the hydraulic grade line, and a dimensionless conveyance factor  $K_f$  (plotted on the right axis, inverted).

### *Conveyance Factor*

The conveyance factor  $K_f$  provides researchers with the ability to quantify how well a particular flow is conveyed through a given conduit by simply examining the aggregate friction slope  $S_f$  for a given depth and flow combination. For pressurized pipes, the factor is computed as  $K_f = 1/\sqrt{S_f} = 1/\sqrt{h_f/\Delta x}$  which is simply the inverse of the square root of the head differential  $h_f$  divided by the length of the pipe  $\Delta x$ . For open-channel conduits, the factor is computed as  $K_f = 1/\sum \sqrt{S_f}$  which corresponds to the aggregated friction losses along a gradually varied flow profile. The derivation of this relationship begins with Manning’s equation and is given as follows:

$$Q = \frac{k_s}{n} AR^{\frac{2}{3}} \sqrt{S_f} = K \sqrt{S_f}; \quad (11)$$

$$\frac{K}{Q} = \frac{1}{\sqrt{S_f}} \equiv K_f, \quad (12)$$

where  $k_s$ ,  $n$ ,  $A$ , and  $R$  are defined in the *Hydraulic Performance Graph* section. The friction slope  $S_f = \Delta h/\Delta x$  where  $\Delta h$  is the change in water surface depth over a given distance  $\Delta x$ .

Smaller conveyance factors correspond to reduced conveyance. By performing this analysis, researchers are able to determine that junction J and pipe JC are a conveyance bottleneck. Using the conveyance factor, the analysis also reveals that the downstream portion of the pipe BJ is not a conveyance bottleneck, even if it is pressurized.

[Figure 3 about here.]

### *Long-term storage performance*

Large-scale combined sewer overflow (CSO) remediation projects are designed to capture CSO events during storms and store the overflows for pumping and treatment after storm events. Large storm events can typically be captured by such systems, but a practical question arises: what is the long-term volumetric performance of such systems? ICAP excels at performing such analyses and performs computations for entire years in a matter of minutes (see Table 2). Researchers modeled the storage performance of an entire year of a system designed to capture combined sewer overflows over a large metropolitan area. Inflows were generated by the Illinois Urban Hydrologic Model (Cantone and Schmidt, 2011) from precipitation records for an entire year. Varied pumping rates based on realistic scenarios were modeled and the effect of different pumping rates on the head in the reservoir is given in Figure 4. Using this volumetric analysis, pumping and inflow regulation strategies can be developed to allow optimization of the operating rules to maximize the ability of the system to convey and store consecutive events.

[Figure 4 about here.]

### *Validation*

To validate the accuracy of the model, results were compared to results generated by the EPA SWMM 5 hydraulic model, using identical topology and inflows. For the SWMM 5 simulation, the model utilized the

dynamic wave routing model including inertial terms, a one-second conduit lengthening step and a one second routing time step. Comparison of results show that for most cases, the ICAP model performs well. In Figure 5, ICAP matches nodal depths well, with a maximum percent error of 8% (relative to the maximum head differential). The behavior of Node B in that figure is due to changes in flow regime. Conditions are oscillating between subcritical, supercritical and pressurized in downstream conduits, and small oscillations can cause jumps between regimes (Hamam and McCorquodale, 1982; Schmidt. et al., 2005). Comparing flow rates in Figure 6, ICAP flows peak sooner than the flow hydrographs do in the SWMM simulation, which is attributable to the temporal assumptions made in ICAP. Most of the differences between the two models occur early in the simulation when the system is filling; this is primarily due to the configuration of the system with the main pipe, JC, having an adverse slope. Finally, run-times of the models are comparable for short-term simulations (for example, five days); on a desktop PC the SWMM simulation completed in 56 seconds vs. ICAP in 86 seconds. SWMM's smaller simulation time is attributed to the setup of interpolation coefficients within ICAP for the HPGs. For long-term simulations (for example, one year), SWMM completed a simulation in one hour and 51 minutes while ICAP completed it in five minutes and 35 seconds.

[Table 2 about here.]

[Figure 5 about here.]

[Figure 6 about here.]

ICAP overestimates depths during unsteady flows (e.g., the rising limb of storm events). A stepwise steady analysis means computed flow will lead the actual flow; the peak flow also does not diffuse, which would in reality occur due to the time of travel of the water. This is also seen as the hydrograph starts to fall: the diffusion of the peak flow does not occur in ICAP, translating into decreasing flow rates earlier than in the dynamic wave model. Since ICAP conserves mass, the error goes to zero as the flow returns to a steady condition. While results compare well in general, the ICAP model is not intended for simulation of unsteady storm events. A dynamic wave model, such as SWMM, is both more precise and more efficient for simulating peak flow and head during unsteady flow events. However, for examining system bottlenecks, capacity, pumping rates, and for simulating long-term events, ICAP provides nearly identical results at much greater efficiency.

## Conclusions

The procedure and program outlined in this work provides researchers with a step-wise steady hydraulic model for free-surface and pressurized pipe flow. The reliance on the hydraulic performance graph for accurate flow routing in a reach provides an excellent understanding of the hydraulic behavior of a conduit network. The ICAP software program is a tool for analyzing the conveyance and long-term volumetric behavior of a closed-conduit system such as a sewer network. The procedures compare well with existing models, and are implemented in the ICAP user interface to provide the user with an easy-to-use, computationally efficient tool for performing such analyses.

## Acknowledgments

This research was conducted under a research grant from the Metropolitan Water Reclamation District of Greater Chicago and was originally designed to be applied to the Tunnel and Reservoir Plan (TARP). The authors are greatly appreciative for the public release of U.S. EPA's SWMM 5 source code which provided a useful graphical user interface for interacting with the conveyance analysis code. Soli deo gloria.

## References

- Bahkmeteff, B. A. (1932). *Hydraulics of Open Channels*. McGraw-Hill.
- Brunner, G. W. (2010). *HEC-RAS Hydraulic Reference Manual, 4.1, January 2010*. U.S. Army Corps of Engineers, Hydrologic Engineering Center, Davis, CA, United States, January 2010 edition.
- Cantone, J. and Schmidt, A. R. (2011). Improved understanding and prediction of the hydrologic response of highly urbanized catchments through development of the Illinois Urban Hydrologic Model. *Water Resources Research*, 47.
- Chow, V. T. (1959). *Open-Channel Hydraulics*. McGraw-Hill.
- Chow, V. T., Maidment, D., and Mays, L. W. (1988). *Applied Hydrology*. McGraw-Hill.
- Danish Hydraulics Institute (2009). *Danish Hydraulics Institute MOUSE pipe flow reference manual*.
- Franz, D. D. and Melching, C. S. (1997). Full Equations (FEQ) model for the solution of the full, dynamic equations of motion for one-dimensional unsteady flow in open channels and through control structures. Water-Resources Investigations Report 96-4240, U.S. Geological Survey.
- Gibson, N. L., Gifford-Miears, C., Leon, A. S., and Vasylykivska, V. S. (2014). Efficient computation of unsteady flow in complex river systems with uncertain inputs. *International Journal of Computer Mathematics*, 91(4):781–797.
- González-Castro, J. and Yen, B. C. (2000a). Applicability of the hydraulic performance graph for unsteady flow routing. Hydraulic Engineering Series 64, University of Illinois, Department of Civil & Environmental Engineering.
- González-Castro, J. and Yen, B. C. (2000b). Open-channel capacity determination using hydraulic performance graph. *Journal of Hydraulic Engineering*, 126:112–122.
- Hager, W. H. (1999). *Wastewater Hydraulics: Theory and Practice*. Springer.
- Hamam, M. A. and McCorquodale, J. A. (1982). Transient conditions in the transition from gravity to surcharged sewer flow. *Canadian Journal of Civil Engineering*, 9:189–196.
- Henderson, F. M. (1966). *Open Channel Flow*. MacMillan Publishing Co.
- Hoy, M. A. (2005). Unsteady flow routing using predetermined solutions to the equations for conservation of mass and momentum. Master’s thesis, University of Illinois at Urbana-Champaign, Department of Civil and Environmental Engineering, University of Illinois, Urbana, IL, United States.
- Landry, B. J. and Oberg, N. (2016). HPG-Util: a software tool for developing hydraulic performance graphs using HEC-RAS. Manuscript in preparation.
- Leon, A. S., Kanashiro, E. A., and Gonzalez-Castro, J. (2013). Fast approach for unsteady flow routing in complex river networks based on performance graphs. *Journal of Hydraulic Engineering*, 139(3):284–295.
- Leon, A. S., Kanashiro, E. A., Valverde, R., and Sridhar, V. (2014). Dynamic framework for intelligent control of river flooding: Case study. *Journal of Water Resources Planning and Management*, 140(2):258–268.
- Oberg, N., Bondar, C., Hoy, M., and Schmidt, A. R. (2006). Conveyance analysis of Chicago’s “Deep Tunnel” system. In *World Environmental and Water Resource Congress*.

- Rossman, L. A. (2008). *Storm Water Management Model User's Manual Version 5.0*. Water Supply and Water Resources Division, National Risk Management Research Laboratory, United States Environmental Protection Agency. EPA/600/R-05/040.
- Schmidt, A. R. (2002). *Analysis of Stage-Discharge Relations for Open-Channel Flows and their Associated Uncertainties*. PhD thesis, University of Illinois at Urbana-Champaign.
- Schmidt, A. R., Ghidaoui, M. S., Leon, A. S., and García, M. H. (2005). Review of sewer surcharging phenomena and models. In *Proceedings of XXXI IAHR Congress*, pages 257–258.
- Tibbetts, J. (2005). Combined sewer systems: Down, dirty, and out of date. *Environmental Health Perspectives*, 113(7):A464–A467.
- U.S. EPA (2016). Combined Sewer Overflows (CSOs). <http://www.epa.gov/npdes/combined-sewer-overflows-csos>.
- Wallingford Software (2002). *Hydraulic Theory, InfoWorks User Manual version 5.5*. Wallingford Software, Wallingford Software, Fort Worth, TX, United States.
- Xia, R. and Yen, B. C. (1992). Sensitivity of flood routing models to variations of momentum equation coefficients and terms. Hydraulic Engineering Series 41, University of Illinois, Department of Civil & Environmental Engineering.
- Yen, B. C. and González-Castro, J. (1994). Determination of Boneyard Creek flow capacity by hydraulic performance graph. Research Report 219, Water Resources Center, University of Illinois at Urbana-Champaign, Water Resources Center, University of Illinois at Urbana-Champaign, Urbana, IL, United States.
- Yen, B. C. and Mays, L. W. (2001). *Hydraulics of Sewer Systems in Stormwater Collection Systems Design Handbook*. McGraw-Hill.
- Zimmer, A., Schmidt, A. R., Ostfeld, A., and Minsker, B. (2013). New method for the offline solution of pressurized and supercritical flows. *Journal of Hydraulic Engineering*, 139:935–948.

## List of Figures

1	Example HPG for channel with a mild characteristic. Each HPC corresponds to a given flow; flow units are in $ft^3/s$ . . . . .	14
2	The ICAP graphical user interface is easy-to-use and includes ability to view results in a number of ways. . . . .	15
3	(a) Plan view of pipe system, where circles indicate inflow locations; point A is the highest inflow location and point C is the storage reservoir. (b) Profile view of hydraulic grade line; flow is from left (point A) to right (point B). Additionally shown in red is the conveyance factor computed for each pressurized pipe. . . . .	16
4	Comparison of head in reservoir for two different pumping scenarios. The solid line on the upper plot represents a pumping rate of $193.4 ft^3/s$ [125 MGD; $5.48 m^3/s$ ]; the dashed line represents a pumping rate of $400 ft^3/s$ [ $11.3 m^3/s$ ]. The lower plot illustrates the total inflow to the system. . . . .	17
5	Comparison of depth at nodes C, J, and B. SWMM results are shown as a dashed line while the solid line represents ICAP results. Secondary axis shows maximum percent error (MPE), relative to maximum water depth. . . . .	18
6	Comparison of flows in pipes AB, BJ, and JC. SWMM results are shown as a dashed line while the solid line represents ICAP results. Secondary axis shows maximum percent error (MPE), relative to maximum normal flow. . . . .	19

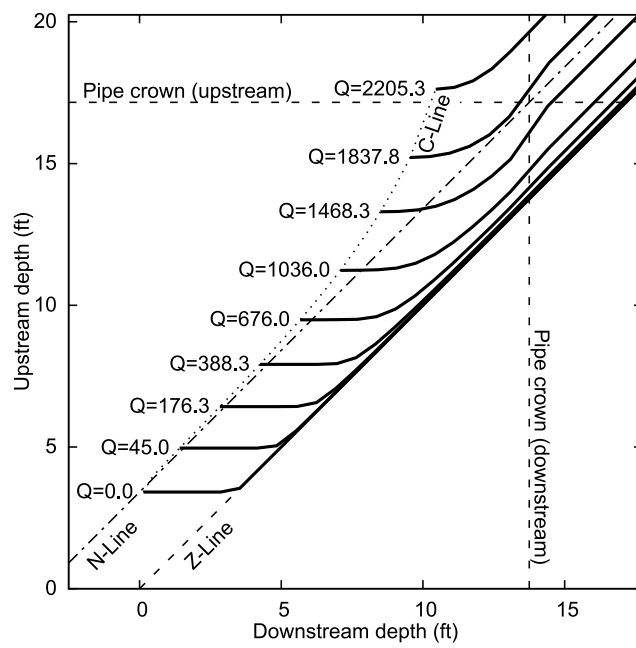


Figure 1: Example HPG for channel with a mild characteristic. Each HPC corresponds to a given flow; flow units are in  $ft^3/s$ .

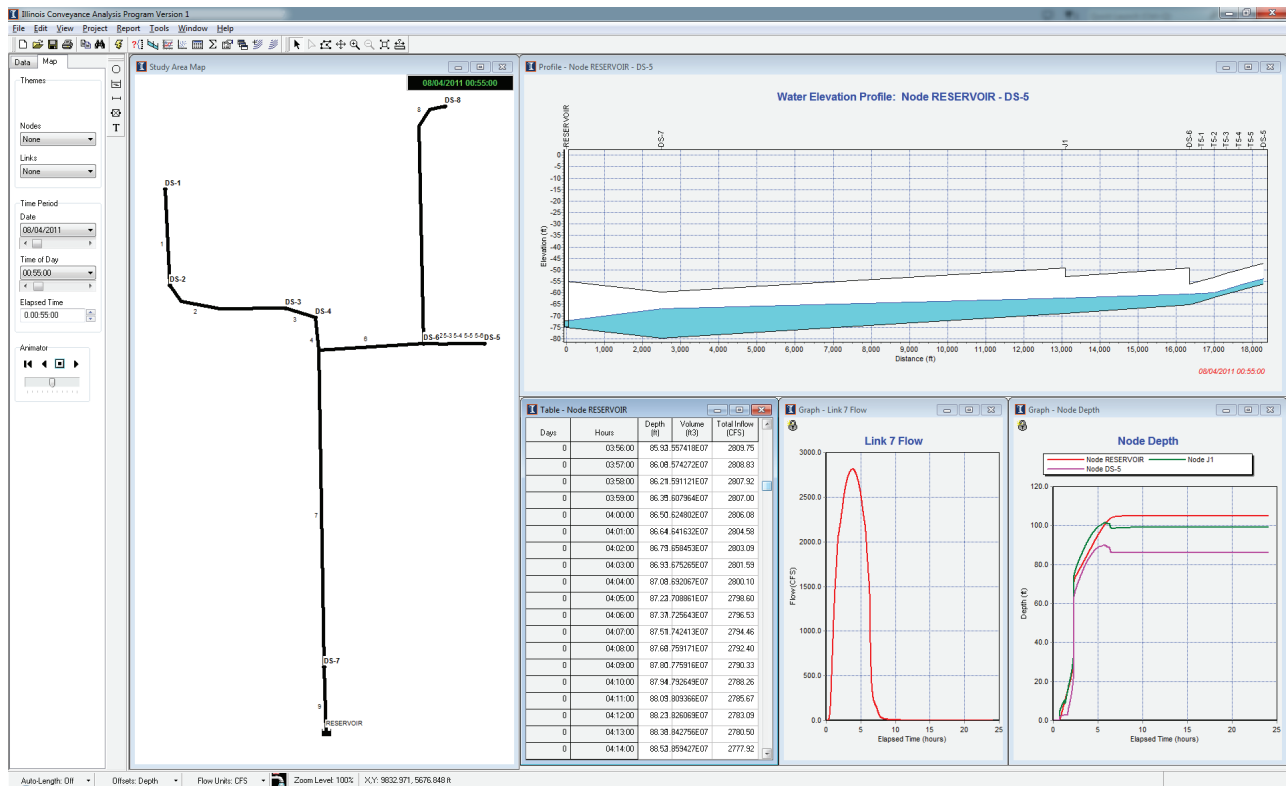


Figure 2: The ICAP graphical user interface is easy-to-use and includes ability to view results in a number of ways.

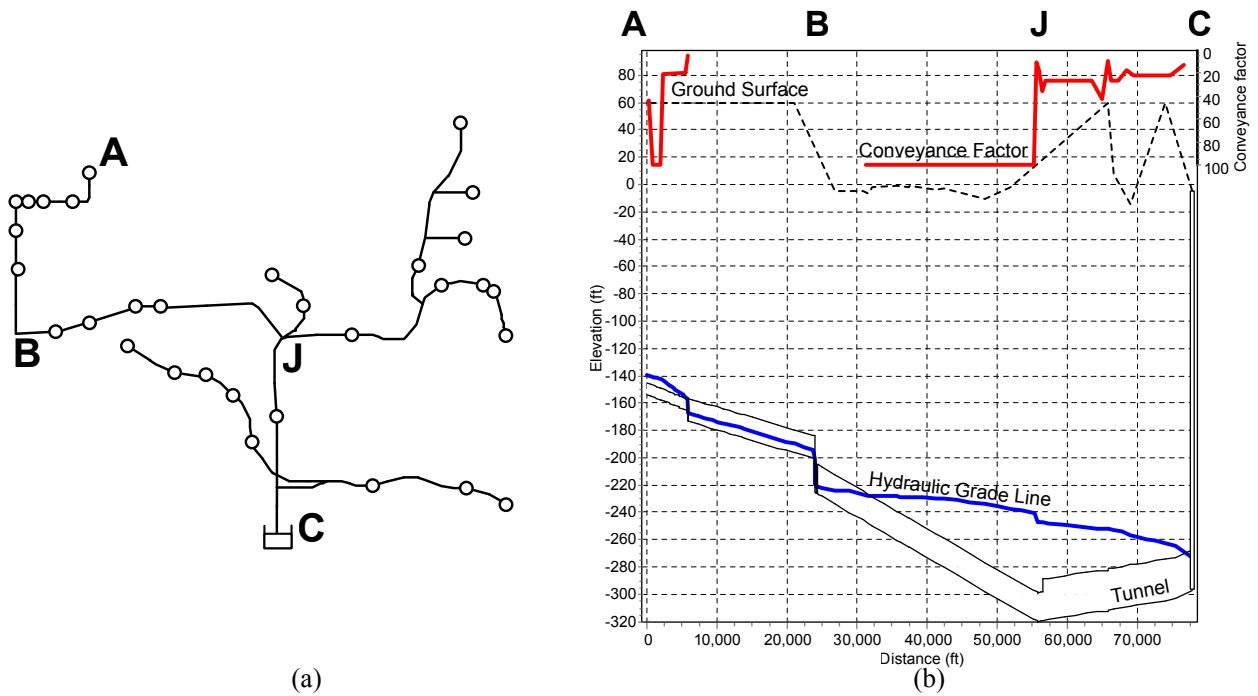


Figure 3: (a) Plan view of pipe system, where circles indicate inflow locations; point A is the highest inflow location and point C is the storage reservoir. (b) Profile view of hydraulic grade line; flow is from left (point A) to right (point B). Additionally shown in red is the conveyance factor computed for each pressurized pipe.



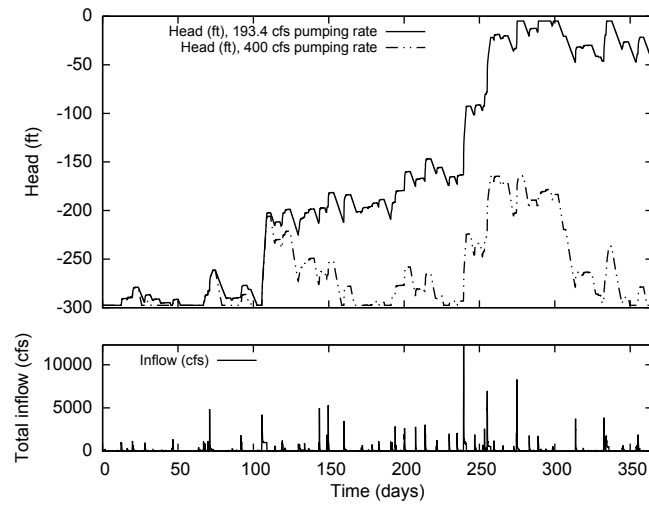


Figure 4: Comparison of head in reservoir for two different pumping scenarios. The solid line on the upper plot represents a pumping rate of  $193.4 \text{ ft}^3/\text{s}$  [125 MGD;  $5.48 \text{ m}^3/\text{s}$ ]; the dashed line represents a pumping rate of  $400 \text{ ft}^3/\text{s}$  [ $11.3 \text{ m}^3/\text{s}$ ]. The lower plot illustrates the total inflow to the system.

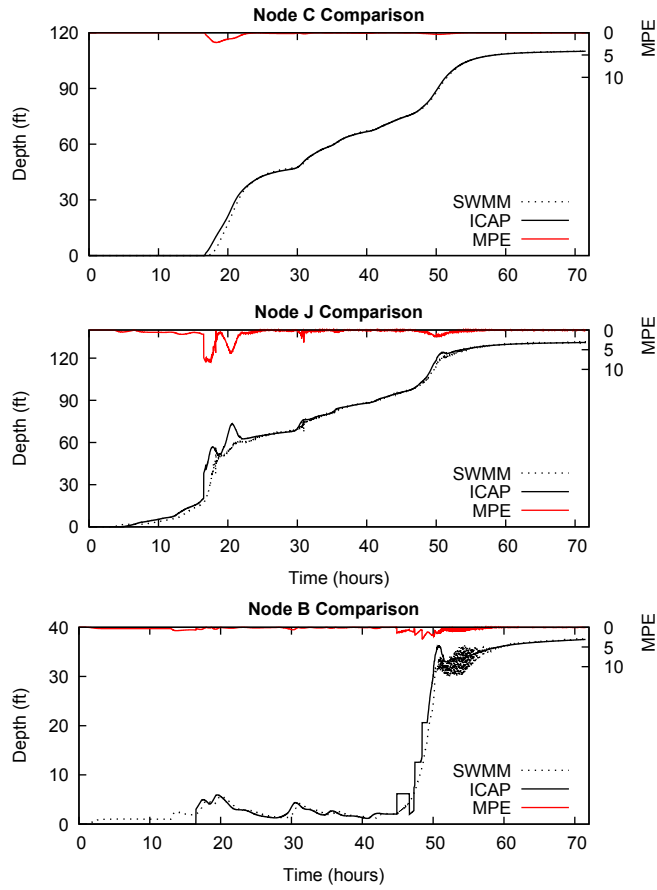


Figure 5: Comparison of depth at nodes C, J, and B. SWMM results are shown as a dashed line while the solid line represents ICAP results. Secondary axis shows maximum percent error (MPE), relative to maximum water depth.

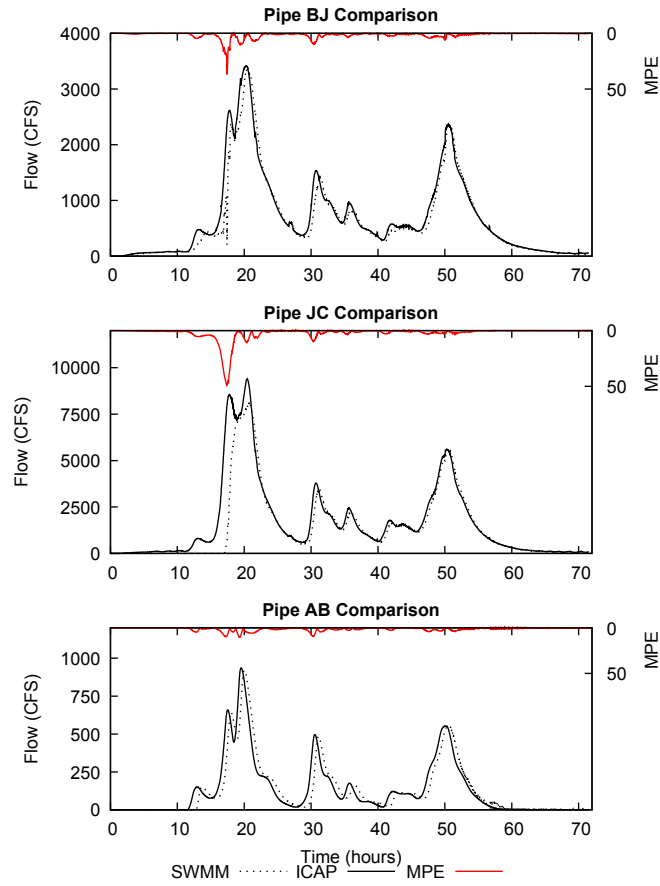


Figure 6: Comparison of flows in pipes AB, BJ, and JC. SWMM results are shown as a dashed line while the solid line represents ICAP results. Secondary axis shows maximum percent error (MPE), relative to maximum normal flow.

## List of Tables

1	Listing of flow/depth conditions and related computations. $Q_l$ and $Q_u$ are the flow rates corresponding to the curves that bracket the input flow $Q$ . The upstream depth on the C-line is represented by $y_{c\text{-line},Q}$ for a flow $Q$ . . . . .	21
2	Computational results for SWMM and ICAP . . . . .	22

<i>Condition</i>	<i>Computation</i>
<b>Subcritical</b> mild adverse horizontal	<b>if</b> $y_{\text{down}} \geq y_{c\text{-line},Q}$ <b>then</b> $y_{\text{up}} = \text{HPG}(Q, y_{\text{down}})$ <b>else</b> $y_{\text{up}} = y_{c\text{-line},Q}$
<b>Subcritical</b> steep	<b>if</b> $y_{\text{down}} \geq y_{c\text{-line},Q_u}$ <b>then</b> $y_{\text{up}} = \text{HPG}(Q, y_{\text{down}})$ <b>else</b> <b>if</b> $y_{\text{down}} \leq y_{c\text{-line},Q}$ <b>then</b> $y_{\text{up}} = y_{c\text{-line},Q}$ <b>else</b> $y_{\text{up}} = \frac{\text{HPG}(Q_l, y_{\text{down}}) + y_{c\text{-line},Q}}{2}$
<b>Pressurized</b>	$y_{\text{up}} = \text{HPG}(Q, y_{\text{down}})$
<b>Supercritical</b>	$y_{\text{up}} = y_{c\text{-line},Q}$

Table 1: Listing of flow/depth conditions and related computations.  $Q_l$  and  $Q_u$  are the flow rates corresponding to the curves that bracket the input flow  $Q$ . The upstream depth on the C-line is represented by  $y_{c\text{-line},Q}$  for a flow  $Q$ .

<b>Simulation Duration</b>	<b>Computation Time</b>	
	<b>ICAP</b>	<b>SWMM</b>
5 days	86s	56s
1 year	5.6m	111m

Table 2: Computational results for SWMM and ICAP